

ORIGINAL
RESEARCH

J.A. Carrillo
A. Lai
P.L. Nghiemphu
H.J. Kim
H.S. Phillips
S. Kharbanda
P. Mofitkhar
S. Lalaezari
W. Yong
B.M. Ellingson
T.F. Cloughesy
W.B. Pope



Relationship between Tumor Enhancement, Edema, *IDH1* Mutational Status, *MGMT* Promoter Methylation, and Survival in Glioblastoma

BACKGROUND AND PURPOSE: Both *IDH1* mutation and *MGMT* promoter methylation are associated with longer survival. We investigated the ability of imaging correlates to serve as noninvasive biomarkers for these molecularly defined GBM subtypes.

MATERIALS AND METHODS: MR imaging from 202 patients with GBM was retrospectively assessed for nonenhancing tumor and edema among other imaging features. *IDH1* mutational and *MGMT* promoter methylation status were determined by DNA sequencing and methylation-specific PCR, respectively. Overall survival was determined by using a multivariate Cox model and the Kaplan-Meier method with a log rank test. A logistic regression model followed by ROC analysis was used to classify the *IDH1* mutation and methylation status by using imaging features.

RESULTS: *MGMT* promoter methylation and *IDH1* mutation were associated with longer median survival. Edema levels stratified survival for methylated but not unmethylated tumors. Median survival for methylated tumors with little/no edema was 2476 days (95% CI, 795), compared with 586 days (95% CI, 507–654) for unmethylated tumors or tumors with edema. All *IDH1* mutant tumors were nCET positive, and most (11/14, 79%) were located in the frontal lobe. Imaging features including larger tumor size and nCET could be used to determine *IDH1* mutational status with 97.5% accuracy, but poorly predicted *MGMT* promoter methylation.

CONCLUSIONS: Imaging features are potentially predictive of *IDH1* mutational status but were poorly correlated with *MGMT* promoter methylation. Edema stratifies survival in *MGMT* promoter methylated but not in unmethylated tumors; patients with methylated tumors with little or no edema have particularly long survival.

ABBREVIATIONS: CI = confidence interval; GBM = glioblastoma multiforme; *IDH1* = isocitrate dehydrogenase-1; IQR = interquartile range; *MGMT* = O-6-methylguanine-DNA-methyltransferase; OR = odds ratio; nCET = non-contrast enhancing tumor; PCR = polymerase chain reaction; ROC = receiver operator curve

GBMs are the most aggressive and lethal primary brain tumors.¹ Standard therapy for GBM is maximal tumor resection with radiation therapy and temozolomide treatment. This is commonly followed by antiangiogenic therapy with bevacizumab at recurrence.² GBM can arise de novo or from degeneration of lower grade tumors (secondary GBM).³ Mutations in the citric acid cycle enzyme *IDH1* have recently been implicated in gliomagenesis and are found in approximately 70%–80% of secondary glioblastomas but are much more rare (<10%) in primary GBMs.^{4–8} *IDH1* mutations are associated with a distinct gene expression profile⁹ (in particular, the proneural subset of malignant gliomas) and are considered an independent prognostic indicator in these patients.^{9,10} Epigenetic silencing of the DNA repair enzyme *MGMT* is another molecular feature of GBM that has both prognostic and pre-

dictive significance because methylation is associated with better outcomes as well as response to temozolomide therapy.¹¹

In addition to molecular signatures, several MR imaging-derived features of GBM also correlate with length of survival. For instance, multiple studies have shown that edema and necrosis are associated with poor outcomes.^{12–14} Other imaging features have been shown to be potentially prognostic in patients with gliomas, including cysts,¹⁵ enhancement,^{12,16,17} multifocality,¹² and location.^{18,19} Some of these imaging features, such as multifocality,²⁰ enhancement,²¹ location,¹⁸ and edema,²² have known molecular correlates.²³ We hypothesized that some of these imaging features reflect differences in molecular signatures such as mutation of *IDH1* or *MGMT* promoter methylation. Therefore, we analyzed the ability of these potentially prognostic imaging features derived from standard MR imaging sequences to predict *IDH1* mutational status and *MGMT* promoter methylation, to develop noninvasive easily acquired biomarkers of these important molecular subtypes of GBM.

Materials and Methods

Patients

All patients participating in this retrospective study signed institutional review board–approved informed consent, agreeing to participation in a study of imaging analysis and clinical outcomes. Outcome

Received July 8, 2011; accepted after revision October 11.

From the Departments of Neurology (J.A.C., A.L., P.L.N., S.L., T.F.C.), Radiological Sciences (H.J.K., B.M.E., W.B.P.), and Pathology and Laboratory Medicine (W.Y.), David Geffen School of Medicine at University of California, Los Angeles, Los Angeles, California; Departments of Neurological Surgery (H.S.P., S.K.) and Radiology (P.M.), University of California, San Francisco, San Francisco, California; and Department of Translational Oncology (H.S.P., S.K.), Genentech, San Francisco, California.

Please address correspondence to Whitney B. Pope, MD, PhD, Department of Radiological Sciences, David Geffen School of Medicine at UCLA, 10833 Le Conte Ave, BL-428 CHS, Los Angeles, CA 90095-1721; e-mail: wpope@mednet.ucla.edu

<http://dx.doi.org/10.3174/ajnr.A2950>

Table 1: Baseline characteristics

	Bevacizumab			
	No (N = 61)	Up-Front (N = 69)	Recurrence (N = 72)	All (N = 202)
Age (yr) (mean)	55.7 ± 13.0	56.8 ± 9.2	56.0 ± 12.6	56.2 ± 11.6
Age range (yr)	23–79	31–72	25–77	23–79
Male (%)	40 (66%)	38 (55%)	36 (50%)	114 (56%)
Median survival (days ± IQR) ^a	628 (± ^c)	588 (± 356)	752 (± 1023)	553 (± 507)
Gross total resection (yes/no) (%) in yes ^a	28/33 (46%)	27/42 (39%)	41/31 (57%)	96/106 (48%)
Methylation (M ¹ /U ² /X ³) ^b	24/36/1	24/45/0	26/35/11	74/116/12
IDH1 mutant/wild type	7/54	4/65	3/69	14/188
nCET (yes/no) (%) in yes	20/41 (32%)	22/47 (35%)	21/51 (33%)	63/139 (32%)
Edema (no, mild/moderate, severe) (%) in no or mild)	28/33 (46%)	22/47 (32%)	23/49 (32%)	73/129 (36%)

Note:—M indicates methylated; U, unmethylated; X, unknown.

^a P = .10 among 3 bevacizumab groups.

^b P = .65 for the only-methylated-versus-unmethylated group.

^c Undefined 75% due to censoring; 25% survival was 293 days.

data from some subsets of these patients have been previously published.^{24,25} Data acquisition was performed in compliance with all applicable Health Insurance Portability and Accountability Act regulations. Patients were selected from the neuro-oncology data base of our institution on the basis of the following criteria: 1) pathology-confirmed GBM based on modified World Health Organization grading system, 2) baseline (presurgical) MR imaging scan, 3) age ≥18 years, and 4) treatment including radiation therapy and temozolomide. Of the 202 patients, 96 had gross total resection, 94 had subtotal resection, and 12 had biopsy only (based on standard imaging). Cases included those associated with a previously published study.²⁶ Follow-up scans were obtained at approximately 4- to 6-week intervals. Steroid doses for patients at the time of initial scanning were not available in most cases. The study spanned 1999–2009. At the time of last assessment (May 2010), 140 of the 202 patients (69%) had died. Most patients in the study received bevacizumab as part of their treatment (186/202, 92%). This was administered “up-front,” that is, 3–6 weeks after tumor resection concurrent with radiation therapy and temozolomide, or they received bevacizumab at tumor recurrence.²⁷ Baseline patient data are shown in Table 1, segregated into groups on the basis of bevacizumab treatment.

Imaging Acquisition

MR imaging was performed on 1.5T or 3T scanners and typically included axial T1-weighted (TR, 400 ms; TE, 15 ms; section thickness, 5 mm), T2-weighted fast spin-echo (TR, 4000 ms; TE, 126–130 ms; section thickness, 5 mm), and gadodiamide- (Omniscan; GE Healthcare, Little Chalfont, Buckinghamshire, United Kingdom; 0.1 mmol/kg) or gadopentetate dimeglumine-enhanced (Magnevist; Bayer Healthcare Pharmaceuticals, Montville, New Jersey; 0.1 mmol/kg) axial and coronal T1-weighted images (TR, 400 ms; TE, 15 ms; section thickness, 3 mm), with an FOV of 24 cm and a matrix size of 256 × 256. Postcontrast images were acquired immediately following contrast injection.

Scoring Imaging Features

Tumors were assessed for size, enhancement, nCET, necrosis, edema, cysts, multifocality, contact with ventricles or neocortex, and location based on prior work,¹² by a neuroradiologist (W.B.P.) blinded to molecular and clinical data as well as outcomes. Briefly, moderate/severe edema was defined as edema extending >1 cm from the margin of the tumor on T2-weighted images; otherwise edema was scored as little, or if absent, none. nCET was graded as positive or negative (for

Kaplan-Meier analysis) and was also qualified as none; minimal; approximately 25%, 50%, 75%; or almost all or all (for the ROC analysis, see below), as judged by the reader (W.B.P.). Nonenhancing tumor was defined as areas of intermediate T2-weighted hyperintensity, less than the intensity of CSF, and corresponding to a region of T1-weighted hypointensity, which was associated with mass effect and architectural distortion, including blurring of the gray-white junction and/or expansion of the deep nuclei, and which showed no obvious enhancement. This method was shown to have high interobserver agreement in a prior study.²¹ Size was determined on the basis of postcontrast T1-weighted images and was measured in longest dimension in centimeters. Enhancement was scored positive for tumors that demonstrated unequivocal increased signal intensity on T1-weighted images following intravenous contrast administration. “Multifocal tumors” were defined as having >1 area of tumor separated by normal brain signal intensity on T2-weighted images. If a secondary lesion fell within the T2-weighted signal-intensity change of the dominant nodule, then the lesion was classified as a “satellite lesion.” “Necrosis” was defined as a region or regions of peripheral and irregular enhancement surrounding areas of high T2-weighted signal intensity. A “cystic tumor” was defined as having an area with peripheral/rim enhancement measuring >1 cm in diameter, demonstrating a thin uniform wall with central high T2-weighted signal intensity approximating that of CSF. “Location” was defined as centered in the frontal, parietal, temporal, occipital, insula or within the posterior fossa, or confined to the deep nuclei (basal ganglia/thalamus). Large tumors that were not clearly centered in a single lobe were scored by the lobes involved (frontal-temporal, frontal-parietal, and so forth).

Molecular Analysis

MGMT promoter methylation status was available for 190 patients and was determined from formalin-fixed paraffin-embedded tissue samples, as previously described.¹⁶ IDH1 mutation was determined by genomic sequencing analysis to identify brain tumor samples containing either wild-type IDH1 or mutations altering amino acid R132. Genomic DNA was isolated from 50–100 mg of brain tumor tissue by using standard methods and a PCR was used to amplify a 295 base pair fragment of the genomic DNA that contains both the intron and second exon sequences of human IDH1, allowing assignment of mutation status assessed by standard molecular biology techniques.

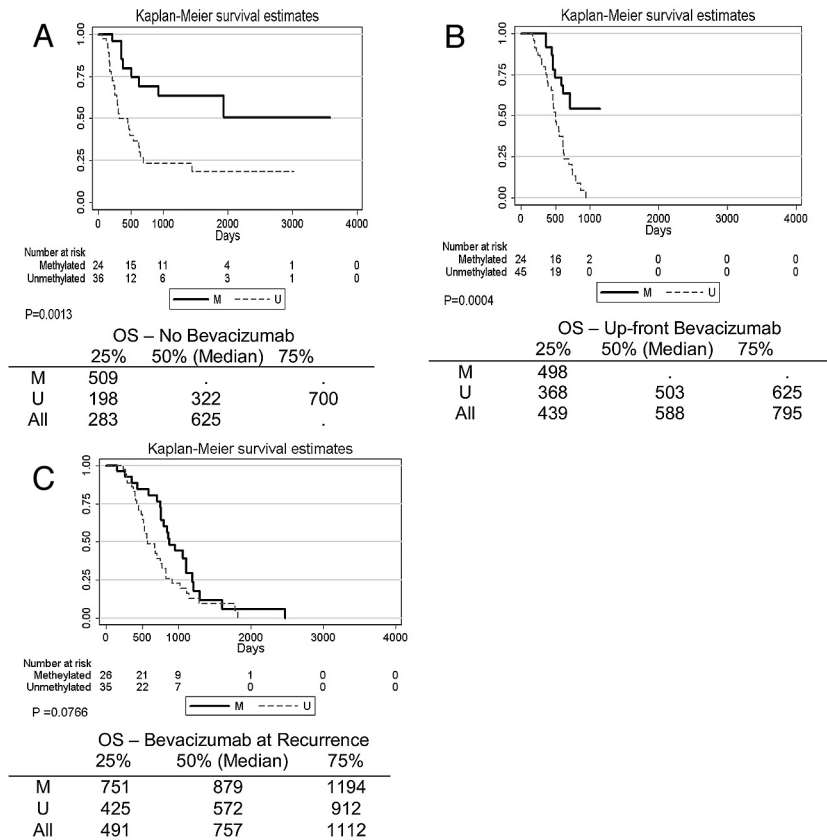


Fig 1. Methylation status stratifies survival in patients not treated with bevacizumab (A) and in patients treated with bevacizumab concurrent with radiation-temozolomide (B). C, A similar pattern is seen in patients treated with bevacizumab at recurrence, though this did not reach statistical significance.

Statistical Methods

Overall survival from the time of tumor resection was recorded, and the median survival with the IQR and the mean patient age with the SD were generated. A test of the proportional hazards assumption was used after fitting a multivariate Cox model, which included MR imaging-derived imaging features, *MGMT* promoter methylation status, *IDH1* mutation status, age, and then the corresponding 95% CIs were generated. The Kaplan-Meier method with the log rank test was used to estimate overall survival on the basis of *MGMT* promoter methylation status (also stratifying by nCET and edema) and *IDH1* mutation status. The level of significance for Kaplan-Meier plots with >2 survival curves represents the overall comparison (based on the log rank test), indicating that at least 1 group is statistically different from the other groups, when P is <.05. A recursive partitioning analysis was used to compare survival on the basis of methylation status and edema.

To compare each clinical and imaging feature between 2 groups from the recursive analysis, we performed a t test or Wilcoxon rank sum test for continuous variables, depending on the distribution (normal versus not), and a χ^2 test for categorical variables. The Spearman ρ correlation coefficient was calculated to characterize the association between tumor location and the *MGMT* promoter methylation/*IDH1* mutational status. A multiple logistic regression analysis was performed for molecular types by using imaging features as covariates. A backward variable selection was used with a significance threshold of 0.1 to model *IDH1* status, and then ROC analysis was performed to evaluate the model by using an area under the curve analysis. Robustness of the model for classifying *IDH1* status was con-

firmed with 20,000 replication bootstrapping, and the bias-corrected 95% CI was reported. For all analyses, a P value of <.05 was accepted as significant. Statistical analysis was performed with STATA (Stata-Corp, College Station, Texas).

Results

MGMT promoter methylation was found in 74/190 (39%) patients. *MGMT* promoter methylation status was associated with better survival ($P < .0001$, log rank test). This relationship was true regardless of whether patients never received bevacizumab ($P = .0013$) or received bevacizumab up-front ($P = .0004$). Methylation status also appeared to stratify survival in patients who received bevacizumab at recurrence, though this did not meet statistical significance ($P = .077$, Fig 1). Adding nCET to methylation status in the Kaplan-Meier analysis appeared to further stratify survival (Fig 2), though the results were not statistically significant in a pair-wise analysis (ie, overall there was a difference in survival curves, but when comparing selected pairs of subgroups, P values were >.05). However, when edema was used to stratify survival, patients with methylated tumors but without edema lived significantly longer than patients with unmethylated tumors or methylated tumors with edema (Fig 3). Using a recursive partitioning analysis for *MGMT* promoter methylation status, we found that methylated tumors without edema had a median survival of 2476 days (95% CI, 1065 not reached), compared with methylated tumors with edema (762 days; 95% CI, 610–953), unmethylated tumors without edema (552 days; 95% CI,

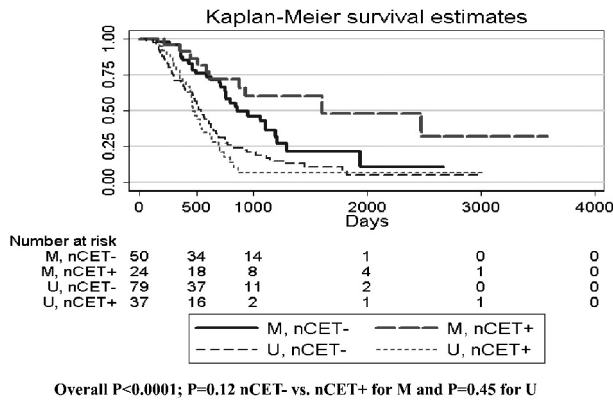


Fig 2. Kaplan-Meier curves for methylated-versus-unmethylated tumors stratified by nCET. The overall P value represents the overall comparison by log rank test, indicating that at least 1 group is different from the others.

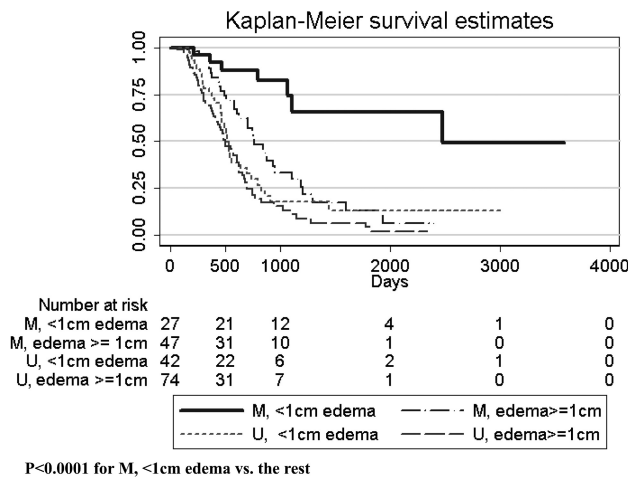


Fig 3. Kaplan-Meier analysis for patients ($n = 190$) with known methylation status, stratified by edema levels. Note that methylated tumors without significant edema have much longer survival than either unmethylated tumors or methylated tumors with edema.

464–702), and unmethylated tumors with edema (501 days; 95% CI, 412–623).

The difference in survival between methylated tumors without edema and the remainder (2476 versus 586 days, $P < .0001$) was not due to age or extent of resection, which was not significantly different between the 2 groups. The only difference between the 2 groups (methylated tumors without edema versus the remainder) in imaging features was that the methylated tumors without edema were slightly smaller (unidimensional largest diameter mean was 4.2 cm for methylated tumors with little/no edema versus 5.1 cm for remainder tumors, t test, $P = .019$). Methylation status was mildly correlated with the presence of multifocal tumors and tumors with satellite lesions (-0.17 , $P = .023$ and 0.18 , $P = .012$, respectively, χ^2 test) but did not correlate with any of the other imaging features. Using a multiple logistic regression analysis, we found that imaging features were only a little better than chance (66% accuracy) at predicting methylation status.

Of 202 tumors, 63 (31%) were nCET+. There was an inverse correlation between nCET+ and edema ($r = -0.36$; $P < .0001$; OR, 0.34; $P < .001$) as previously shown.¹² Multifocality, which is thought to be associated with poor outcomes,¹² was less common for methylated compared with unmethyl-

ated tumors (OR, 0.20; $P = .038$) but was more common among nCET+ compared with nCET- tumors (OR, 7.94; $P = .001$).

IDH1 mutation was present in 14/202 (6.9%) tumors, and was associated with longer survival ($P = .002$, log rank test). All *IDH1* tumors were nCET+ (Fig 4). Most *IDH1* tumors (11/14, 79%) involved the frontal lobe versus 69/188 (37%) wild type tumors, as reported previously for this dataset.²⁶ Thus the OR for frontal lobe involvement for mutant versus wild type was 6.3 (95% CI, 1.7–23.5). The *IDH1* mutation was not an independent predictor of survival in a multivariate analysis that included imaging features and methylation status (Table 2). This is likely due to the association of the *IDH1* mutation with *MGMT* promoter methylation (OR for methylated tumors versus unmethylated tumors being *IDH1* mutants: 3.07, $P = .053$; Spearman $\rho = 0.15$, $P = .044$). Methylation status was available for all 14 *IDH1* mutant tumors. Of these, 9 (64%) were found to be methylated.

To test whether imaging could predict *IDH1* status, we performed a logistic regression analysis by using all imaging features as covariates. A higher percentage of nCET, larger size of tumor, presence of cysts, and presence of satellites all correlated with *IDH1* mutant tumors by using a backward variable selection with a threshold of 0.1. The area under the curve for *IDH1* mutational status was 0.94 (Fig 5) with bootstrap bias-corrected 95% CI, 0.85–0.99. Accuracy was 97.5% with a sensitivity of 71.4% and a specificity of 99.5% (note that bootstrap bias-corrected 95% CIs were 95.0%–100%, 42.9%–100%, and 97.8%–100% for accuracy, sensitivity, and specificity, respectively).

Discussion

Imaging correlates of gene expression may provide important insight into subtypes of GBM. For example, Pope et al²¹ compared gene expression in completely-versus-incompletely enhancing tumors and found overexpression of genes associated with hypoxia, angiogenesis, and edema in the former. Similarly, Van Meter et al²⁸ and Diehn et al²⁹ examined genes that were differentially expressed on the basis of contrast enhancement and areas of central necrosis, again noting upregulation of genes associated with angiogenesis within areas of contrast enhancement. Barajas et al³⁰ analyzed the relationship between gene expression and radiographic images, including physiologic imaging techniques such as perfusion and diffusion MR imaging, showing that regions of tumor with high blood volume and/or low apparent diffusion coefficient express gene profiles associated with angiogenesis and tumor aggressiveness. In contrast to angiogenic gene expression associated with edema, necrosis, and shortened survival, the *IDH1* mutation and *MGMT* promoter methylation status define molecular subtypes of glioblastoma with a favorable prognosis. We hypothesized that these molecular signatures may be reflected in imaging features derived from standard MR imaging. Therefore, we analyzed the relationship between MR imaging features and these GBM subtypes in a large cohort of patients as a first step in developing noninvasive biomarkers of these groups that may be useful, particularly when tissue-based testing is inconclusive or not possible.

As previously shown,³¹ both the *IDH1* mutation and *MGMT* promoter methylation were associated with longer

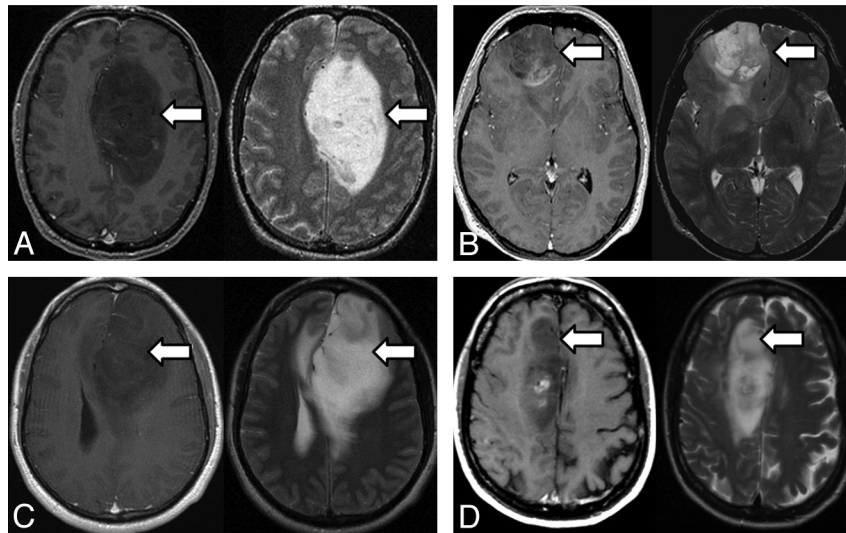


Fig 4. A–D, Four examples of *IDH1* mutant tumors on MR imaging. For each set of paired images, T1 postcontrast images on the left are shown with the corresponding T2-weighted image on the right. Note abundant nonenhancing tumor (arrows) and frontal lobe location.

Table 2: Multivariate analysis of molecular markers and imaging features in relationship to survival^a

Variable	HR	Standard Error	P Value	95% CI
Methylated	0.4	0.08	<.001	0.3–0.6
Moderate edema	1.7	0.34	.009	1.1–2.5
Multifocal	2.4	0.76	.005	1.3–4.5
Age at treatment ^b	1.3	0.13	.006	1.1–1.6
<i>IDH1</i> mutation	0.5	0.23	.142	20–1.3

Note:—HR indicates hazard ratio.

^aGlobal test of proportional hazards: $P = .17$.

^bStandardized age at treatment.

survival. *MGMT* promoter methylation has been associated with susceptibility to temozolomide treatment.¹¹ Temozolomide is 1 of 3 medications approved by the FDA for the treatment of glioblastoma, in addition to carmustine³² and, more recently, the anti-angiogenic agent bevacizumab.² All the patients in the current study received temozolomide, so the response to this treatment based on methylation status could not be tested. However, we did find that methylation status stratified survival, regardless of bevacizumab therapy.

In a multivariate analysis, we found that *MGMT* promoter methylation was prognostic of better outcome, but *IDH1* status was only significant in a univariate analysis. There are 2 likely reasons why *IDH1* status was not independently prognostic in the multivariate model. One is that there was a strong correlation between *IDH1* mutation and *MGMT* promoter methylation as others have previously found.³³ Second, the *IDH1* mutation is relatively rare in GBM because it is associated with secondary but not primary tumors.⁷ We found that only 6.9% of tumors in our cohort were *IDH1*-mutated, similar to the incidence in a previous report.³¹ Thus the low number of *IDH1* mutants and strong correlation with *MGMT* promoter methylation may explain the lack of independent impact on prognosis in the multivariate analysis.

As for imaging features, edema and multifocality were associated with poor outcome, as previously demonstrated.^{12,34} Rim enhancement has been reported to be associated with unmethylated primary GBM, whereas a mixed-nodular en-

hancement pattern was associated with methylated and secondary GBM.^{23,35,36} We did not find a significant difference in edema levels or tumor location between methylated and unmethylated tumors, similar to findings in prior reports.^{35,36} However, we did find that edema was able to stratify survival in methylated but not in unmethylated tumors. Thus edema levels may be particularly important for patient prognosis in the *MGMT* promoter methylated tumor subset.

MGMT promoter methylation is more common in the proneural than the mesenchymal subset of GBM.³³ Proneural tumors have a better prognosis than other glioblastoma subtypes.^{37,38} It may also be that tumors with little or no edema also are more likely to fall within the proneural subset, but this hypothesis has not been formally tested, to our knowledge. Previous reports have shown that MR imaging texture can predict *MGMT* promoter methylation status with fairly high accuracy (71%).³⁵ We did not perform a texture analysis. We did not find any imaging features that correlated well with *MGMT* promoter methylation, so it seems that predicting methylation status from MR imaging without postprocessing analyses or advanced imaging techniques may be challenging.

Results from the current study suggest that imaging features could be used to predict *IDH1* mutation with 97.5% accuracy. Although this needs to be confirmed in a large prospective trial, these results suggest that simple imaging features might be able to serve as a useful biomarker of *IDH1* status. For example, all *IDH1* mutant tumors were nCET+, and most *IDH1* tumors involved the frontal lobe. Because increased vascular endothelial growth factor levels are associated with vascular permeability³⁹ and hence contrast enhancement, the presence of large regions of nonenhancing tumor in *IDH1* mutants implies that this molecular genotype has low vascular endothelial growth factor levels, in contrast to a prior report.⁴⁰ The frontal lobe predilection for *IDH1* tumors is notable. There is some precedent for lobar specificity for molecular subtypes of glioma. For instance, in oligodendrogliomas, 1p19q-deleted tumors also appear to be more common in the frontal lobe,⁴¹ and some have suggested that insular oligodendrogliomas are rarely or never 1p19q-deleted,⁴² though this

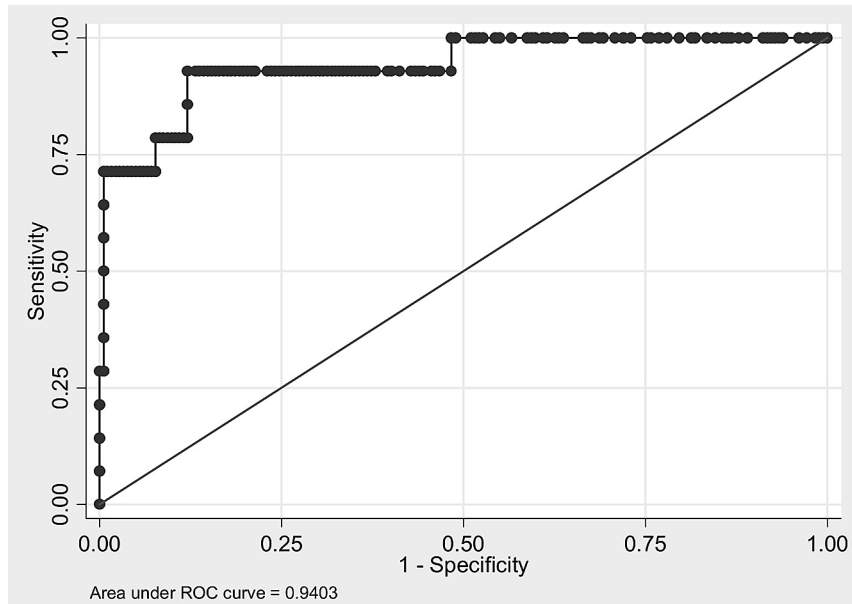


Fig 5. ROC analysis of imaging features used to predict *IDH1* mutational status. Combining percentage nCET, tumor size, cyst, and satellites allows a 94% accuracy in classifying tumors in this test set with 14 *IDH1* mutants.

finding is controversial.⁴³ GBMs have varying amounts of oligodendroglioma component, and this pathologic finding is associated with 1p19q deletions and better outcome.^{44,45} Thus it would be of interest to see if there is a relationship between an oligodendroglioma component with the 1p19q codeletion and the *IDH1* mutation.

Our analysis is limited by its retrospective nature. In particular, our model of imaging features that can predict *IDH1* mutational status will need to be confirmed in a prospective test set of patients. Also, it is possible that the relationship between imaging features and survival is dependent on treatment paradigms, which are constantly evolving. Steroid dose, which can affect edema and enhancement, was not available for many of our patients. Distinguishing edema from nonenhancing tumor can be challenging in some cases. Timing of contrast administration also could affect the classification of nonenhancing tumor because the proportion of tumor that enhances can increase as the time between contrast injection and scanning increases. However, most of the *IDH1* mutants had large areas of nonenhancing tumor, potentially diminishing this limitation. Although the ability to identify nonenhancing tumor with high interobserver reliability has previously been demonstrated,⁴⁶ the single-reader methodology used also is a limitation of this study. Approximately half of our patients received subtotal resection, and 12 had biopsy only. Therefore, it is possible that sampling error could lead to underestimation of the *IDH1* mutation incidence. However, it seems that in most patients, the *IDH1* mutation tends to be present in all or most tumor cells, potentially mitigating the impact of this issue.^{24,25,27}

Conclusions

We confirmed that *MGMT* promoter methylation and *IDH1* mutation are associated with longer survival. Patients with methylated tumors with little or no peritumoral edema had particularly long survival. Standard MR imaging features may

be able to accurately predict *IDH1* mutational status but are poorly predictive of *MGMT* promoter methylation.

Disclosures: Albert Lai—RELATED: Grant: Roche,* Genentech,* Consulting Fee or Honorarium: Roche, Genentech, UNRELATED: Consultancy: Roche, Genentech, Grants/Grants Pending: Roche,* Genentech,* Merck,* Schering Plough.* Heidi Phillips—UNRELATED: Employment: Genentech, Stock/Stock Options: Genentech, Roche. Samir Kharbada—UNRELATED: Employment: Genentech; Stock/Stock Options: Genentech. Timothy Cloughesy—UNRELATED: Consultancy: Genentech, Roche, Agios, Lilly, Novartis, Payment for Lectures (including service on Speakers Bureaus): Merck. Whitney Pope—UNRELATED: Consultancy: Genentech, Payment for Lectures (including service on Speakers Bureaus): Genentech, Payment for Development of Educational Presentations: Genentech. (*Money paid to the institution.)

References

- Norden AD, Drappatz J, Wen PY. Antiangiogenic therapies for high-grade glioma. *Nat Rev Neurol* 2009;5:610–20
- Cohen MH, Shen YL, Keegan P, et al. FDA drug approval summary: bevacizumab (Avastin) as treatment of recurrent glioblastoma multiforme. *Oncologist* 2009;14:1131–38
- Ohgaki H, Kleihues P. Genetic alterations and signaling pathways in the evolution of gliomas. *Cancer Sci* 2009;100:2235–41
- Bals J, Meyer J, Mueller W, et al. Analysis of the *IDH1* codon 132 mutation in brain tumors. *Acta Neuropathol* 2008;116:597–602
- Bleeker FE, Lamba S, Leenstra S, et al. *IDH1* mutations at residue p.R132 (*IDH1*(R132)) occur frequently in high-grade gliomas but not in other solid tumors. *Hum Mutat* 2009;30:7–11
- De Carli E, Wang X, Puget S. *IDH1* and *IDH2* mutations in gliomas. *N Engl J Med* 2009;360:2248. Author reply 2249
- Parsons DW, Jones S, Zhang X, et al. An integrated genomic analysis of human glioblastoma multiforme. *Science* 2008;321:1807–12
- Yan H, Bigner DD, Velculescu V, et al. Mutant metabolic enzymes are at the origin of gliomas. *Cancer Res* 2009;69:9157–59
- Ducray F, El Hallani S, Idhahbi A. Diagnostic and prognostic markers in gliomas. *Curr Opin Oncol* 2009;21:537–42
- Dubbink HJ, Taal W, van Marion R, et al. *IDH1* mutations in low-grade astrocytomas predict survival but not response to temozolomide. *Neurology* 2009;73:1792–95
- Hegi ME, Diserens AC, Godard S, et al. Clinical trial substantiates the predictive value of O-6-methylguanine-DNA methyltransferase promoter methylation in glioblastoma patients treated with temozolomide. *Clin Cancer Res* 2004;10:1871–74
- Pope WB, Sayre J, Perlina A, et al. MR imaging correlates of survival in patients with high-grade gliomas. *AJNR Am J Neuroradiol* 2005;26:2466–74
- Lacroix M, Abi-Said D, Fourney DR, et al. A multivariate analysis of 416 pa-

- tients with glioblastoma multiforme: prognosis, extent of resection, and survival. *J Neurosurg* 2001;95:190–98
14. Hammoud MA, Sawaya R, Shi W, et al. Prognostic significance of preoperative MRI scans in glioblastoma multiforme. *J Neurooncol* 1996;27:65–73
 15. Utsuki S, Oka H, Suzuki S, et al. Pathological and clinical features of cystic and noncystic glioblastomas. *Brain Tumor Pathol* 2006;23:29–34
 16. Tynninen O, Aronen HJ, Ruhala M, et al. MRI enhancement and microvascular density in gliomas: correlation with tumor cell proliferation. *Invest Radiol* 1999;34:427–34
 17. Chaichana KL, Kosztowski T, Niranjana A, et al. Prognostic significance of contrast-enhancing anaplastic astrocytomas in adults. *J Neurosurg* 2010;113:286–92
 18. Kappadakunnel M, Eskin A, Dong J, et al. Stem cell associated gene expression in glioblastoma multiforme: relationship to survival and the subventricular zone. *J Neurooncol* 2010;96:359–67
 19. Lim DA, Cha S, Mayo MC, et al. Relationship of glioblastoma multiforme to neural stem cell regions predicts invasive and multifocal tumor phenotype. *Neuro Oncol* 2007;9:424–29
 20. Kyritsis AP, Bondy ML, Xiao M, et al. Germline p53 gene mutations in subsets of glioma patients. *J Natl Cancer Inst* 1994;86:344–49
 21. Pope WB, Chen JH, Dong J, et al. Relationship between gene expression and enhancement in glioblastoma multiforme: exploratory DNA microarray analysis. *Radiology* 2008;249:268–77
 22. Carlson MR, Pope WB, Horvath S, et al. Relationship between survival and edema in malignant gliomas: role of vascular endothelial growth factor and neuronal pentraxin 2. *Clin Cancer Res* 2007;13:2592–98
 23. Bruzzone MG, Eoli M, Cuccarini V, et al. Genetic signature of adult gliomas and correlation with MRI features. *Expert Rev Mol Diagn* 2009;9:709–20
 24. Pusch S, Sahm F, Meyer J, et al. Glioma IDH1 mutation patterns off the beaten track. *Neuropathol Appl Neurobiol* 2010;37:428–30
 25. Camelo-Piragua S, Jansen M, Ganguly A, et al. Mutant IDH1-specific immunohistochemistry distinguishes diffuse astrocytoma from astrocytosis. *Acta Neuropathol* 2010;119:509–11
 26. Lai A, Kharbada S, Pope WB, et al. Evidence for sequenced molecular evolution of IDH1 mutant glioblastoma from a distinct cell of origin. *J Clin Oncol* 2011;29:4482–90
 27. Lai A, Tran A, Nghiemphu PL, et al. Phase II study of bevacizumab plus temozolomide during and after radiation therapy for patients with newly diagnosed glioblastoma multiforme. *J Clin Oncol* 2011;29:142–48
 28. Van Meter T, Dumur C, Hafez N, et al. Microarray analysis of MRI-defined tissue samples in glioblastoma reveals differences in regional expression of therapeutic targets. *Diagn Mol Pathol* 2006;15:195–205
 29. Diehn M, Nardini C, Wang DS, et al. Identification of noninvasive imaging surrogates for brain tumor gene-expression modules. *Proc Natl Acad Sci U S A* 2008;105:5213–18
 30. Barajas RF, Hodgson JG, Chang JS, et al. Glioblastoma multiforme regional genetic and cellular expression patterns: influence on anatomic and physiologic MR imaging. *Radiology* 2010;254:564–76
 31. Weller M, Felsberg J, Hartmann C, et al. Molecular predictors of progression-free and overall survival in patients with newly diagnosed glioblastoma: a prospective translational study of the German Glioma Network. *J Clin Oncol* 2009;27:5743–50
 32. Aoki T, Hashimoto N, Matsutani M. Management of glioblastoma. *Expert Opin Pharmacother* 2007;8:3133–46
 33. Noushmehr H, Weisenberger DJ, Diefes K, et al. Identification of a CpG island methylator phenotype that defines a distinct subgroup of glioma. *Cancer Cell* 2010;17:510–22. Epub 2010 Apr 15
 34. Kyritsis AP, Levin VA, Yung WK, et al. Imaging patterns of multifocal gliomas. *Eur J Radiol* 1993;16:163–70
 35. Drabycz S, Roldan G, de Robles P, et al. An analysis of image texture, tumor location, and MGMT promoter methylation in glioblastoma using magnetic resonance imaging. *Neuroimage* 2010;49:1398–405
 36. Eoli M, Menghi F, Bruzzone MG, et al. Methylation of O6-methylguanine DNA methyltransferase and loss of heterozygosity on 19q and/or 17p are overlapping features of secondary glioblastomas with prolonged survival. *Clin Cancer Res* 2007;13:2606–13
 37. Phillips HS, Kharbada S, Chen R, et al. Molecular subclasses of high-grade glioma predict prognosis, delineate a pattern of disease progression, and resemble stages in neurogenesis. *Cancer Cell* 2006;9:157–73
 38. Lee Y, Scheck AC, Cloughesy TF, et al. Gene expression analysis of glioblastomas identifies the major molecular basis for the prognostic benefit of younger age. *BMC Med Genomics* 2008;1:52
 39. Lacerda S, Law M. Magnetic resonance perfusion and permeability imaging in brain tumors. *Neuroimaging Clin N Am* 2009;19:527–57
 40. Zhao S, Lin Y, Xu W, et al. Glioma-derived mutations in IDH1 dominantly inhibit IDH1 catalytic activity and induce HIF-1alpha. *Science* 2009;324:261–65
 41. Kim JW, Park CK, Park SH, et al. Relationship between radiological characteristics and combined 1p and 19q deletion in World Health Organization grade III oligodendroglial tumours. *J Neurol Neurosurg Psychiatry* 2011;82:224–27
 42. Goze C, Rigau V, Gibert L, et al. Lack of complete 1p19q deletion in a consecutive series of 12 WHO grade II gliomas involving the insula: a marker of worse prognosis? *J Neurooncol* 2009;91:1–5
 43. Wu A, Aldape K, Lang FF. High rate of deletion of chromosomes 1p and 19q in insular oligodendroglial tumors. *J Neurooncol* 2010;99:57–64
 44. Klink B, Schlingelhof B, Klink M, et al. Glioblastomas with oligodendroglial component: common origin of the different histological parts and genetic subclassification. *Anal Cell Pathol (Amst)* 2010;33:37–54
 45. Salvati M, Formichella AI, D'Elia A, et al. Cerebral glioblastoma with oligodendroglial component: analysis of 36 cases. *J Neurooncol* 2009;94:129–34
 46. Pope WB, Kim HJ, Huo J, et al. Recurrent glioblastoma multiforme: ADC histogram analysis predicts response to bevacizumab treatment. *Radiology* 2009;252:182–89
 47. Capper D, Zentgraf H, Balss J, et al. Monoclonal antibody specific for IDH1 R132H mutation. *Acta Neuropathol* 2009;118:599–601